Liquid Crystals
Publication details, including instructions for authors and subscription information:
http://www.informaworld.com/smpp/title~content=t713926090

Mesomorphic properties of some 1,4,8,11,15,18,22,25-octa-alkoxymethylphthalocyanines

A. N. Cammidge[a]; M. J. Cook[a]; S. D. Haslam[b]; R. M. Richardson[b]; K. J. Harrison[c]
[a] School of Chemical Sciences, University of East Anglia, Norwich, England [b] School of Chemistry, University of Bristol, Bristol, England [c] DRA Electronics Division, Malvern, England

To cite this Article Cammidge, A. N. , Cook, M. J. , Haslam, S. D. , Richardson, R. M. and Harrison, K. J.(1993) 'Mesomorphic properties of some 1,4,8,11,15,18,22,25-octa-alkoxymethylphthalocyanines', Liquid Crystals, 14: 6, 1847 — 1862

To link to this Article: DOI: 10.1080/02678299308027720

URL: http://dx.doi.org/10.1080/02678299308027720

Liquid Crystals, 1993, Vol. 14, No. 6, 1847–1862

Mesomorphic properties of some 1,4,8,11,15,18,22,25-octa-alkoxymethylphthalocyanines

by A. N. CAMMIDGE and M. J. COOK
School of Chemical Sciences, University of East Anglia, Norwich NR4 7TJ, England

S. D. HASLAM and R. M. RICHARDSON*
School of Chemistry, University of Bristol, Cantock's Close, Bristol BS8 1TS, England

and K. J. HARRISON
DRA Electronics Division, St Andrew's Road, Malvern WR14 3PS, England

The mesophase behaviour of a number of non-peripherally octa-substituted phthalocyanine derivatives has been studied by optical microscopy, differential scanning calorimetry (DSC) and X-ray diffraction. A homologous series of straight chain alkoxymethyl derivatives has exhibited both rectangular and hexagonal columnar mesophases, with the rectangular phases being favoured by the shorter chains. Two branched chain derivatives were found to give rectangular columnar phases at room temperature. A detailed analysis of the X-ray data has shown some differences from the analogous *n*-alkyl compounds. It has been deduced that the increased polarizability and flexibility of the ether linkage allows the disc-like molecules to approach more closely face to face with correspondingly thicker columns.

1. Introduction

The first phthalocyanines reported to exhibit a thermotropic mesophase were octa-substituted at the peripheral (2,3,9,10,16,17,23,24) sites with long chain alkoxymethyl groups [1, 2] (compound series **1** in figure 1). Subsequent work has shown that derivatives similarly substituted with eight alkyl [3, 4] or alkoxy groups [3, 5] (series **2** and **3**) may also develop liquid crystal phases. The more frequently encountered mesophases are the columnar discotic, but branching of the chains can sometimes give rise to cholesteric [6] and nematic discotic [7] behaviour. A different series of liquid crystal phthalocyanines has been developed by Cook *et al.* and these (series **4**) bear eight alkyl groups at the non-peripheral (1,4,8,11,15,18,22,25) positions [8]. Some examples exhibit up to three different columnar mesophases [9] and liquid crystal behaviour has been observed for a metallated compound with chains as short as pentyl [10]. In contrast, a preliminary investigation of the straight chain alkoxy analogues, series **5**, has shown that these do not give rise to a liquid crystal phase. The present work extends our investigations to the metal-free octa-alkoxymethyl derivatives, series **6**, and the two metallated derivatives **7** and **8**, and was undertaken to develop further the comparisons between the peripherally and non-peripherally substituted series. This paper reports the thermal behaviour for the

---

* Author for correspondence.

0267–8292/93 $10·00 © 1993 Taylor & Francis Ltd.

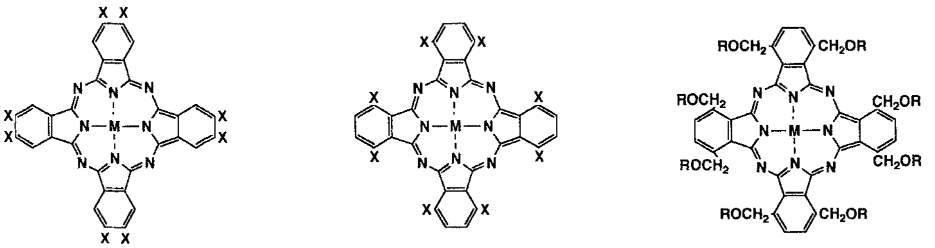

(1) X = $CH_2OAlkyl$, M = H,H or metal

(2) X = Alkyl, M = H,H or metal

(3) X = OAlkyl, M = H,H or metal

(4) X = Alkyl, M = H,H or metal

(5) X = OAlkyl, M = H,H or metal

(6) M = H,H

a R = C_3H_7
b R = C_4H_9
c R = C_5H_{11}
d R = C_6H_{13}
e R = C_7H_{15}
f R = C_8H_{17}
g R = C_9H_{19}
h R = $C_{10}H_{21}$
i R = 2-octyl
j R = 2-ethylhexyl

(7) M = Zn, R = C_7H_{15}

(8) M = Cu, R = C_7H_{15}

Figure 1. Structures of some mesogenic phthalocyanines.

compounds and X-ray diffraction data (excluding derivatives **7** and **8**) obtained from their mesophases. The latter reveal how the molecular packing is dependent on the length of the aliphatic chains.

2. Experimental

2.1.1. *Materials*

The synthesis and spectroscopic characterization of the compounds has been described elsewhere [11].

2.1.2. *Thermotropic behaviour*

The thermotropic behaviour of the compounds was investigated by differential scanning calorimetry (DSC) using a Mettler TA 3000 thermal analyser with a Mettler DSC 30 cell and by optical microscopy using a Vickers polarizing microscope in conjunction with a Mettler FP 52 hot stage.

2.1.3. *X-ray diffraction*

X-ray diffraction measurements were made using copper K_α radiation (wavelength, $\lambda = 1{\cdot}54$ Å) that was monochromated with a pyrolytic graphite crystal and nickel filtered. The X-rays were detected using a two dimensional position-sensitive detector [12]. The unaligned, powder samples were contained within glass Lindemann capillary tubes, but the aligned sample of compound **6i** was contained between two thin (0·008 mm) polyimide (Kapton) films glued to a brass washer. The alignment was obtained by cooling from the isotropic phase into the mesophase at a rate of $10°C\,hr^{-1}$ in the presence of a homogeneous 9 T magnetic field. Due to the small amount available (1–2 mg), sample **6j** was mounted on a pin-head. Hence, it was not possible to investigate the effect of temperature on the structure of the mesophase of this compound. The samples, excluding **6j**, were contained in a heating cell which was controlled by a Eurotherm 818P. A sample to detector distance of 0·890 (±0·002)m was used for the accurate determination of the position of the low angle peaks corresponding to the intercolumnar distance, while 0·190 (±0·001)m was used to survey the diffraction pattern at higher angles. The diffraction data from the powders are presented by averaging the diffracted intensity over all pixels at equal scattering angles (2θ) and plotting against the scattering vector, $\mathbf{Q}$ ($=4\pi \sin \theta/\lambda$).

3. Results and discussion

3.1. *Thermotropic behaviour*

3.1.1. *Straight chain derivatives*

In preliminary experiments, each compound was investigated by both microscopy and DSC up to 300°C. Microscopy revealed that the compounds undergo slow decomposition at temperatures above *c.* 250°C and that none of the compounds melt into an isotropic state below 300°C. The DSC thermogram for the octapropoxymethylphthalocyanine, **6a**, showed no obvious peaks up to 300°C, and analysis by microscopy confirmed that it remained as a crystalline solid at least to the point where decomposition began. However, the longer straight chain homologues all showed liquid crystal behaviour. To avoid problems associated with decomposition, subsequent DSC heating and cooling cycles were undertaken between room temperature and *c.* 180°C. A feature of the series is that each compound showed significant supercooling. Compounds **6b**, **6d** and **6g** gave a single endothermic peak corresponding to the transition C–D and a single peak during the cooling cycle. The remaining compounds gave more complex thermograms with a second endothermic peak on the heating cycle. **6h** also showed an extra peak in the cooling cycle, but the most complex behaviour was exhibited by **6e** which gave three closely spaced peaks on heating and two on cooling (see figure 2). The transition temperatures obtained from the thermograms are listed in table 1. In most cases the second peak (and third in the case of **6e**) appears in the same temperature region as the first. The higher temperature peak has been tentatively assigned to C–D and the lower ones to C–C transitions. These assignments could not be confirmed by optical microscopy, because textures derived from the crystal state were not distinctive. The absence of an I–D transition further hindered characterization of the mesophases.

The X-ray diffraction experiments described in § 3.2. reveal that the heptoxymethyl and octoxymethyl derivatives, **6e** and **6f**, both exhibit two distinct mesophases. For **6e**, these were observed at 90°C and 120°C. However, the DSC thermogram showed no endothermic peak between these temperatures which indicates that the enthalpy for the D–D transition is very low. Similarly, the D–D transition for **6f** must fall between 80°C and 220°C. The DSC trace for this compound showed no endotherm above 67°C in a run which was terminated at 190°C.

The C–D transition temperatures for series **6** are generally lower for the longer chain derivatives and the transition enthalpies higher. Data for the peripherally substituted isomers, **1**, of members of the present series are restricted to the octa-octoxymethyl derivative. This exhibits a single mesophase between 67°C and 320°C, the C–D transition occurring at the same temperature as that for the non-peripherally substituted compound, **6f**. Figure 3 compares the C–D transition temperatures for the present series with corresponding data for the non-peripherally substituted octa-alkylphthalocyanines, series **4** [9]. The *x* axis plots the number of non-hydrogen atoms in the substituent chains of the two series. For shorter chain derivatives, the octa-alkylphthalocyanines melt into the mesophase at lower temperatures, but this trend is reversed for chain lengths longer than eight non-

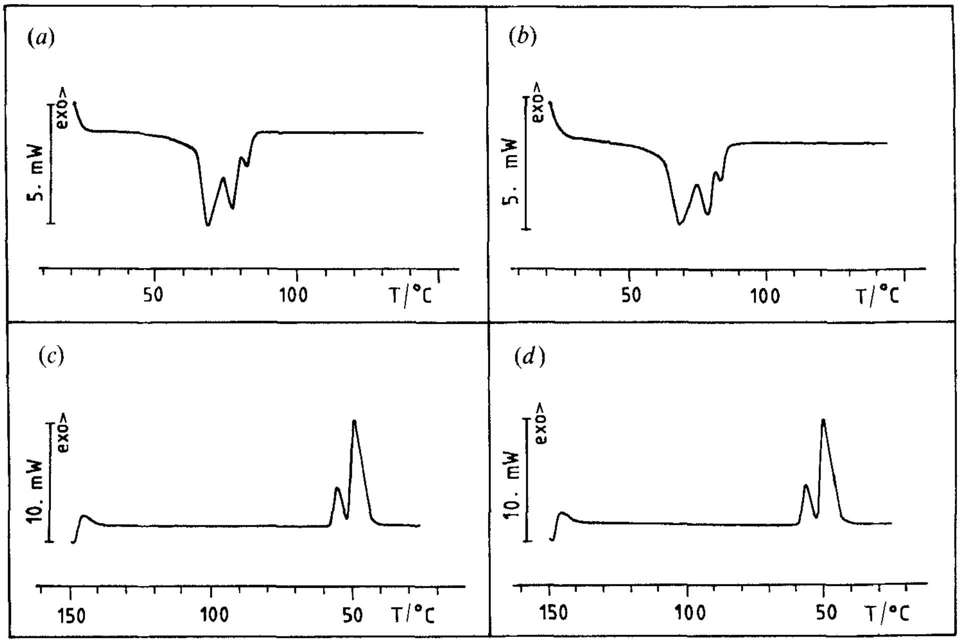

Figure 2. The DSC thermogram for **6e** showing the multiple peaks in the heating and cooling cycles. (*a*) First heating, (*b*) first cooling, (*c*) second heating and (*d*) second cooling.

Table 1. Thermotropic data for some (1,4,8,11,15,18,22,25)-octa-alkoxymethylphthalocyanines **6**, **7** and **8** observed between room temperature and 300°C.

No.	Compound Substituent	M	Heating cycle† C–D	Heating cycle† D–I	ΔH‡	Cooling cycle† D–C
6b	Butoxymethyl	H_2	185	—	6	125
6c	Pentoxymethyl	H_2	123 (81)§	—	7	74
6d	Hexoxymethyl	H_2	85	—	6	46
6e	Heptoxymethyl	H_2	79 (67, 72)‖	—	19¶	55 (50)‖
6f	Octoxymethyl	H_2	67 (62)	—	19	46
6g	Nonoxymethyl	H_2	75	—	27	54
6h	Decoxymethyl	H_2	64 (58)	—	22	45 (39)
6i	2-Octoxymethyl	H_2	—	106	0·7	—
6j	2-Ethylhexoxymethyl	H_2	—	236	2	—
7	Heptoxymethyl	Zn	70 (64)	—	17	64
8	Heptoxymethyl	Cu	82 (69)	—	18	58

† Numbers in parentheses ( ) refer to other peak positions observed on the DSC thermograms but transitions could not be identified by optical polarized microscopy.

‡ In kcal mol^{-1}.

§ The enthalpy of the endotherm at 81° is *c.* 0·5 kcal mol^{-1}.

‖ See figure 1.

¶ The total enthalpy for the three unresolved peaks.

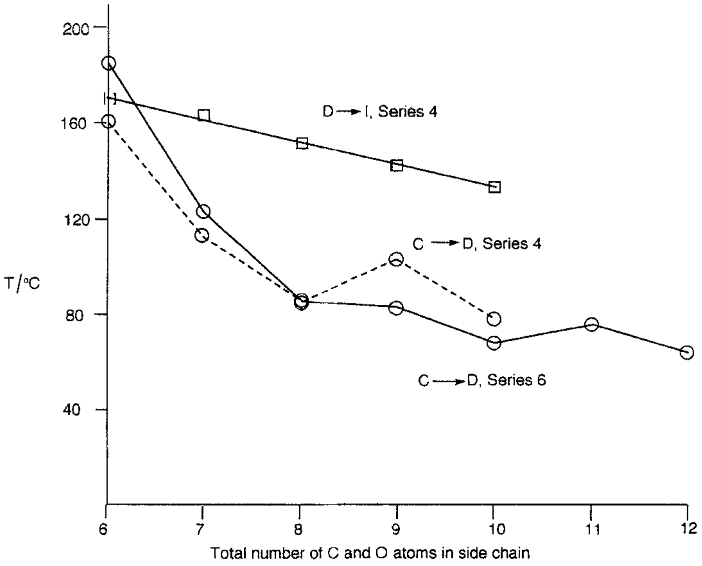

Figure 3. Comparison of the mesophase behaviour of non-peripherally octa-substituted phthalocyanines of series **4** and series **6**. The plots show transition temperatures as a function of chain length for C–D, and D–I transitions, for the former series and the C–D for the latter.

hydrogen atoms. In all cases, the mesophase range of the alkoxymethyl compound is far greater than for their octa-alkyl counterparts.

The effects on the C–D transition resulting from incorporation of a metal ion into **6e** to form the zinc and copper analogues **7** and **8** are summarized in table 1. The presence of the copper ion has little effect, whereas zinc lowers the transition temperature. Earlier results obtained for the metal-free, copper and zinc derivatives of the peripherally substituted octa-dodecoxymethyl derivatives show that copper rather than zinc lowers the transition temperature [2].

3.1.2. *Branched chain derivatives*

The octa-(2-octoxymethyl) and octa-(2-ethylhexoxymethyl) derivatives **6i** and **6j** were obtained as mixtures of diastereoisomers because the synthetic pathway to these products utilized racemic precursors for the side chain components [11]. The materials behave very differently from the straight chain analogues. They are liquid-crystalline at room temperature and no transition was observed under the polarizing microscope down to −20°C or by DSC down to −100°C. Furthermore, both show a transition into the isotropic state at an accessible temperature and with a low transition enthalpy. The birefringent textures observed through the polarizing microscope on cooling from the isotropic liquid were also similar; an example is depicted in figure 4.

There is a further interesting contrast between **6j** and the peripherally substituted metal-free octa-(2-ethylhexoxymethyl)phthalocyanine. The latter does not show a

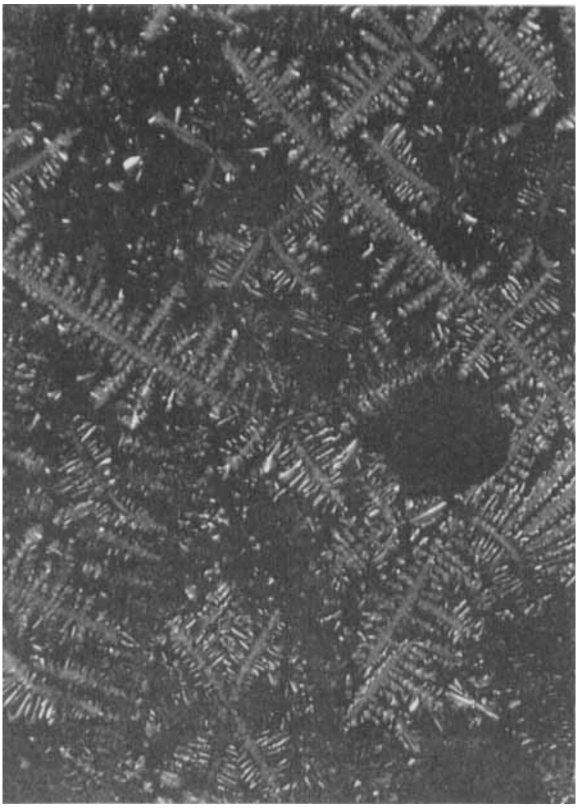

Figure 4. The optical texture observed through the polarizing microscope on cooling **6j** to 25°C from the isotropic liquid.

transition into the columnar mesophase until 170°C (and thereafter a further transition into a discotic nematic mesophase at 223°C [7]). The very much lower C–D transition temperature for **6j** presumably arises because the substituents in the present series are located in sterically more crowded sites and steric hindrance becomes serious when the chains are branched. This causes disruption of the crystal packing and leads to a lower transition temperature.

3.2. *X-ray diffraction from straight chain derivatives*

The alkoxymethyl derivatives, **6b** to **6h**, gave diffraction patterns characteristic of columnar mesophases. It was found that the butoxy, pentoxy and hexoxy homologues (**6b** to **6d**) exhibited the 'rectangular disordered' D_{rd} phase [13]. The heptoxy and octoxy derivatives showed the D_{rd} phase at lower temperatures, but the 'hexagonal disordered' D_{hd} phase on further heating. The longer chain homologues (nonoxy and decoxy) showed only the D_{hd} phase. The identification of these phases, shown schematically in figure 5, from the powder diffraction patterns is discussed in the section below.

These materials could not be aligned magnetically, so the diffraction patterns contain sharp rings which result from the long-range two dimensional ordering of the columns. The rings have been indexed according to a rectangular unit cell. Even

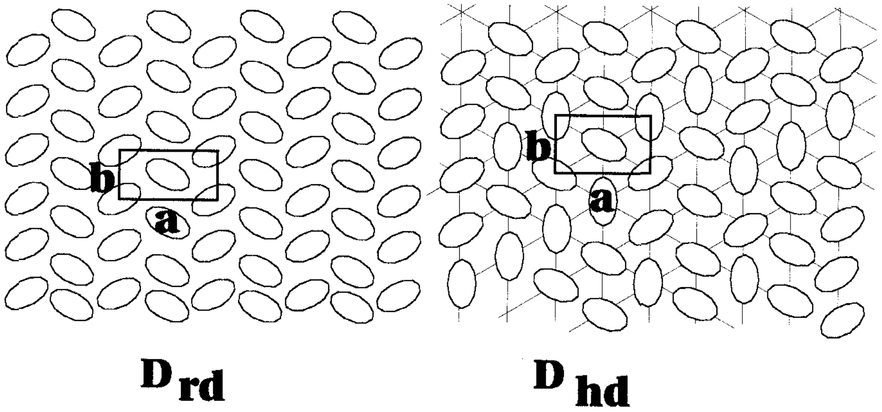

Figure 5. Possible schematic structure of D_{rd} and D_{hd} mesophases showing the unit cells. Each ellipse represents the end of a column of tilted discotic molecules. In the D_{rd} phase there is a herringbone packing of columns. In the D_{hd} the correlation of orientations is short and the lattice becomes hexagonal.

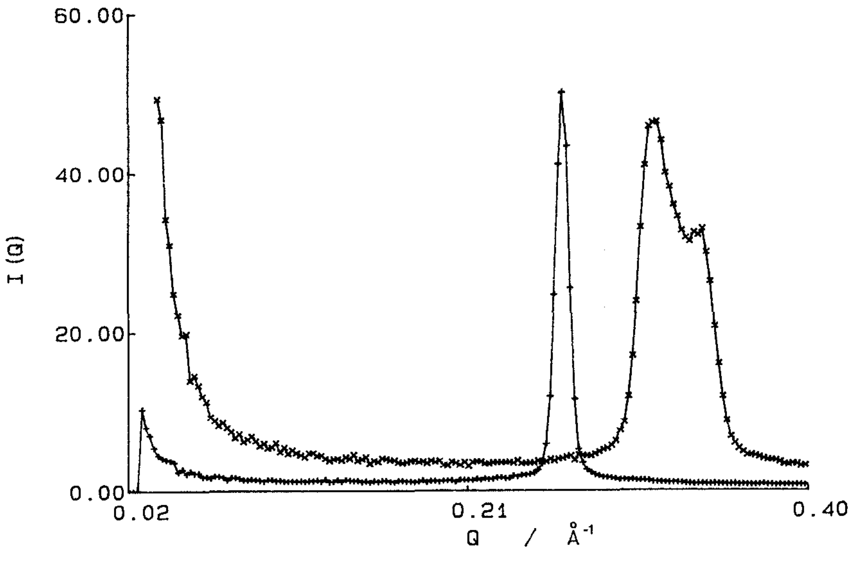

Figure 6. Small angle X-ray scattering from hexagonal and rectangular columnar mesophases. Note the single 200/110 peak from the hexagonal phase and the split peaks from the rectangular phase. (+) Hexagonal phase (octyloxymethyl derivative) and (×) rectangular phase (butyloxymethyl derivative).

with a large sample to detector distance, the 200 and 110 reflections appear as a single diffraction ring for the hexagonal phase, but are split for the rectangular phase. Figure 6 shows an example of each phase and the unit cell dimensions are given in table 2. The reflections at higher angles are consistent with the assignments of D_{rd} or D_{hd}. Figure 7 shows the scattering from the pentoxy derivative (**6c**) at

140°C where the 020/310 and 400/220 peaks are observed in addition to the very strong 110/200 peak.

The rectangular phase has been assigned the D_{rd} structure rather than the D_t structure even though the peaks associated with the non-centred D_{rd} lattice, for example 210s and 120s, appear to be absent. A D_t lattice would distort significantly from the basic hexagonal geometry; only small distortions from the hexagonal geometry are observed (i.e. $a \approx \sqrt{3}b$). The 'non-centred' peaks are probably too weak to be observed. Hence, the rectangular lattices have been assigned the herringbone D_{rd} structure.

The formation of a herringbone lattice as the substituent chain length decreases has also been observed by Weber *et al.* [14] in their investigation of the structures of the 2,3,9,10,16,17,23,24-octa-alkoxymethylphthalocyanines.

It is possible to rationalize the tendency to give rectangular phases for short chain derivatives and hexagonal phases for longer chains as follows. First one postulates that for small substituents the structure of the molecule is similar to that of the unsubstituted phthalocyanine, and so tends to form the same crystal structure. Robertson [15] showed that the unsubstituted molecule adopts a herringbone lattice structure with tilted molecules. This type of packing is very common in aromatic molecules and, according to Kitaigorodsky [16], it is one of the lowest free energy conformations of hard and rigid molecules. The tendency to form a hexagonal 'flat' lattice as the alkoxymethyl chain length increases and as we move away from hard rigid molecules must be explained by an additional contribution to the intermolecular forces.

One effect that would drive the structure towards having discs perpendicular to the columns and hence a hexagonal phase is the tendency for the polarizable cores to pack together, leaving the less polarizable alkyl chains to pack with each other. The polarizability of the core would be enhanced by the oxygen atoms and the formation of a hexagonal lattice would maximize the interaction between 'like' parts of molecules. A hexagonal lattice would also maximize the configurational entropy of the alkyl chains, since a column of tilted discs would allow less free motion of the chain. The oxygen atoms in the chains are thought to give the alkyl groups more freedom to move compared with the methylene groups in the analogous octa-alkyl substituted phthalocyanines [9]. This may help explain the lower temperature phases

Table 2. Lattice parameters for mesophases formed by compounds **6b**–**6h** deduced from X-ray diffraction measurements.

	T/°C	Columnar phase	Lattice parameters (b, ±0·3 Å)
Butoxy	205	D_{rd}	$b=23{\cdot}3$, $a=36{\cdot}4$
Pentoxy	140	D_{rd}	$b=25{\cdot}2$, $a=39{\cdot}9$
Hexoxy	205	D_{rd}	†
Heptoxy	90	D_{rd}	†
	120	D_{hd}	$b=26{\cdot}4$
Octoxy	80	D_{rd}	†
	220	D_{hd}	$b=27{\cdot}6$
Nonoxy	120	D_{hd}	$b=29{\cdot}0$
Decoxy	120	D_{hd}	$b=30{\cdot}2$

† Peak splitting is visible but too small to measure accurately.

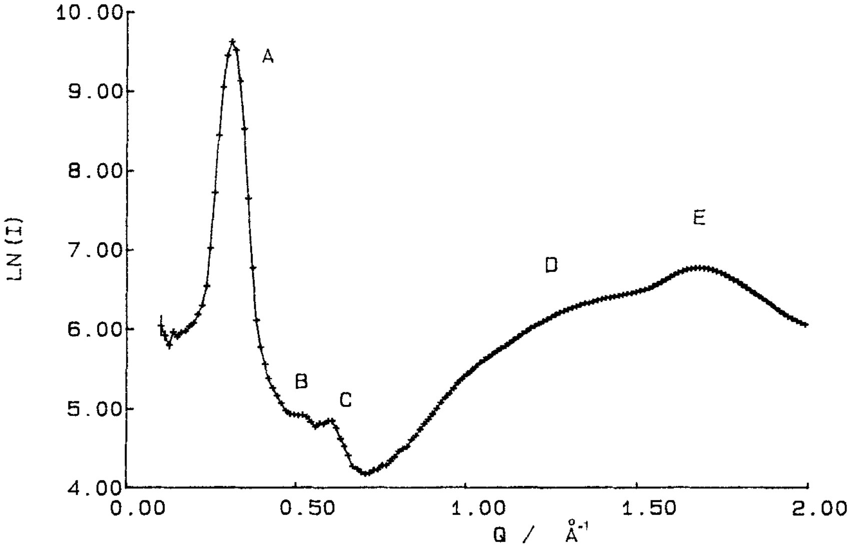

Figure 7. X-ray scattering from compound **6c** at 140°C showing the main features of the diffraction pattern, A, B and C are generated by the rectangular lattice. A, 200/110; B, 020/130; C, 400/220; D, alkyl chain peak (4·7 Å) and E, intracolumnar peak (3·7 Å).

of the alkoxymethyl derivatives, the alkyl groups being able to move more freely than in the octa-alkyl compounds and hence being more 'liquid like'. The oxygen atoms can also allow the alkyl chains to move into the plane of the core, which may explain why the cores can pack so closely in the columns in the hexagonal phase.

Evidence for the ability of the oxygen atom to allow the alkoxy chains to move into the plane of the core can be found by comparing the lattice parameters of the hexagonal phases of the octa-octoxymethyl and the octa-octyl [9] derivatives; $b_{\mathrm{octyloxymethyl}} = 27{\cdot}6$ Å and $b_{\mathrm{octyl}} = 22{\cdot}6$ Å. If we allow for the extra $-CH_2O-$ group in the alkoxymethyl derivative, then the 'adjusted' b_{octyl} will be about 25 Å, still 2 Å shorter than that obtained for the alkoxymethyl analogue. This may be explained by the sterically hindered octyl chains having to move out of the plane of the core, so making the effective column diameter less. This would allow the columns to pack more closely, but would also force the cores apart within the columns. The diffuse, wide-angle scattering peaks provide some evidence that there is indeed a difference in the intermolecular correlations along the column. This is discussed in the paragraph below.

In the octoxymethyl compound, core–core close packing within the columns is observed and exhibits itself in the form of a broad peak in the wide angle region at 3·7 Å ($Q = 1{\cdot}7$ Å^{-1}). This peak appears in all of the mesophases of alkoxymethyl derivatives studied (see figure 8) and is due to short range intra-columnar ordering, 3·7 Å being the perpendicular distance between molecules in the columnar phase. This distance is physically reasonable for the face to face close packing of such aromatic discs. Since the ordering within the columns is only short range, the Q value of this diffuse peak will correspond to the intermolecular distance normal to the cores, not the distance separating the cores along the columnar axis, even if the

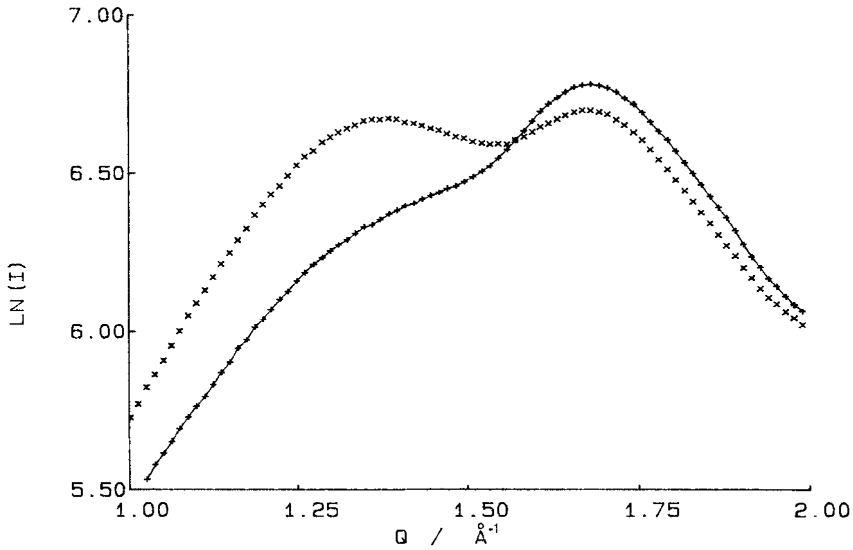

Figure 8. Detail of X-ray scattering from compounds **6c** and **6h** showing diffuse outer peaks. The plot shows the decrease in intensity of the alkyl chain peak with decrease in chain length. (+) Pentoxymethyl derivative and (×) decoxymethyl derivative.

molecules are tilted. Since we do not know the separation along the column we cannot calculate the tilt angle of the molecules with respect to the axis.

The major difference between the alkyl and alkoxymethylphthalocyanines is that the 3·7 Å 'intermolecular' peak is not seen in the diffraction from the alkyl derivatives (see figure 9). This suggests that the perpendicular distance is greater in the alkyl derivatives, so the diffuse peak coincides with the 4·5 Å peak from the alkyl chain packing. This would be consistent with the suggestion that the steric interference between the alkyl chains forces the discs further apart (to *c.* 4–5 Å) while the more flexible alkoxymethyl chains allow them to approach to 3·7 Å.

A second broad peak is observed at 4·7 Å ($Q = 1{\cdot}35\,\text{Å}^{-1}$) in all of the homologues with the exception of the C_4 derivative. Since the intensity of this peak diminishes with the length of the alkyl chain (see figure 8), and since the position of the peak does not move (i.e. *d* spacing does not appear to be a function of chain length) we can assign this peak to the close packing interactions of linear alkyl chains.

X-ray diffraction from liquid *n*-alkanes (as shown in figure 10) yields a broad peak at 4·5 Å [17], the position of which is independent of the length of the molecule and adds further confirmation of the origin of this broad peak in the diffraction pattern of the mesophases.

3.3. *X-ray diffraction from branched chain derivatives*

The magnetically aligned sample of compound **6i** yielded the diffraction pattern shown in figure 11.

Measurement of the peaks occurring at small angles (see figures 12, 13 and table 3) suggests that the mesophase has rectangular symmetry with the lattice parameters given in table 3. The lattice expands slightly upon cooling. This may be explained by the increased rigidity of the alkyl chains as the sample is cooled. The small, yet

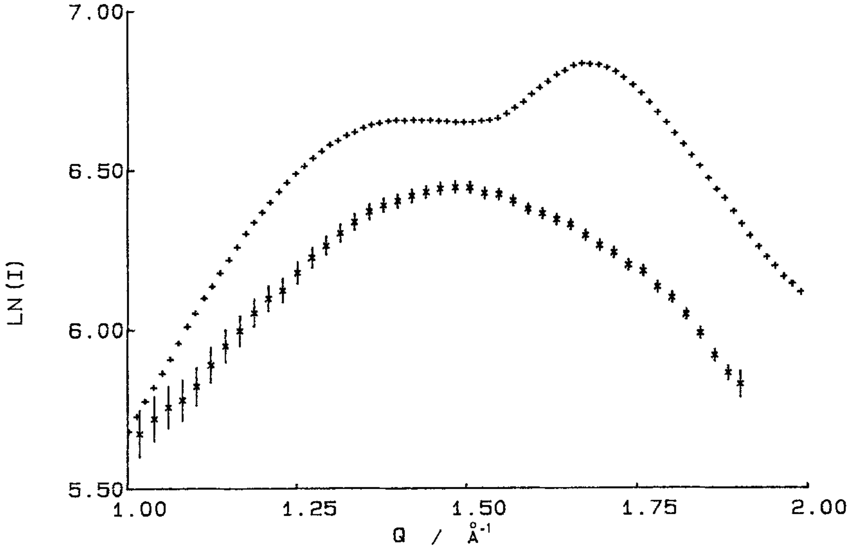

Figure 9. Detail of X-ray scattering from compound **6f** and its octa-octyl analogue (series **4**; $X = C_8H_{17}$). The intracolumnar 3·7 Å peak is clearly visible in the case of the octoxymethyl derivative, but not so in the case of the octyl analogue. (+) Octoxymethyl derivative and (×) octyl derivative.

sharp, peak visible at $Q = 0{\cdot}45\,\text{Å}^{-1}$ in figure 13 has tentatively been indexed as 210 ($Q_{\text{THEORY}} = 0{\cdot}426\,\text{Å}^{-1}$), which would support the idea of a non-centred (herringbone) lattice (see figure 5). It is feasible that the superposition of the 210 peak and the broad background peak associated with the insulating polyimide (Kapton) heating cell windows (see figure 13 (*b*)) would result in an apparent shift of the 210

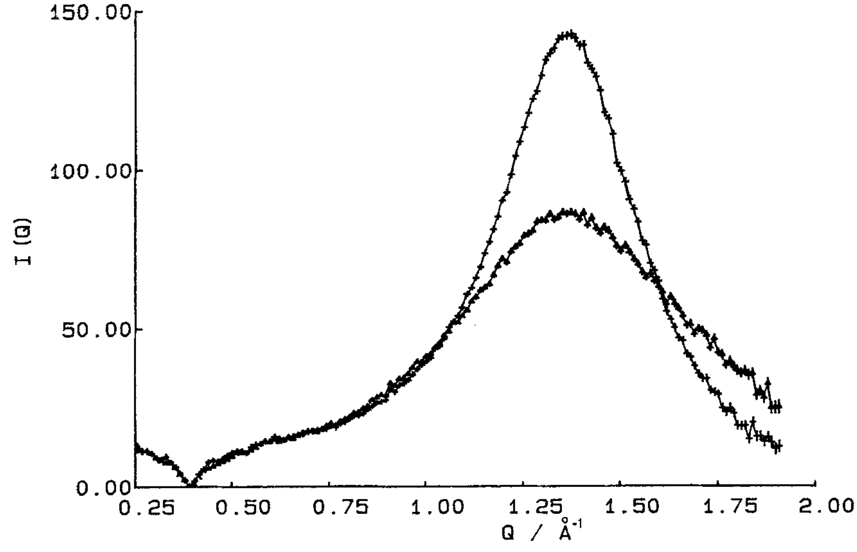

Figure 10. X-ray diffraction from liquid *n*-octadecane and *n*-pentane. (+) Octadecane (40°C) and (▲) pentane (room temperature).

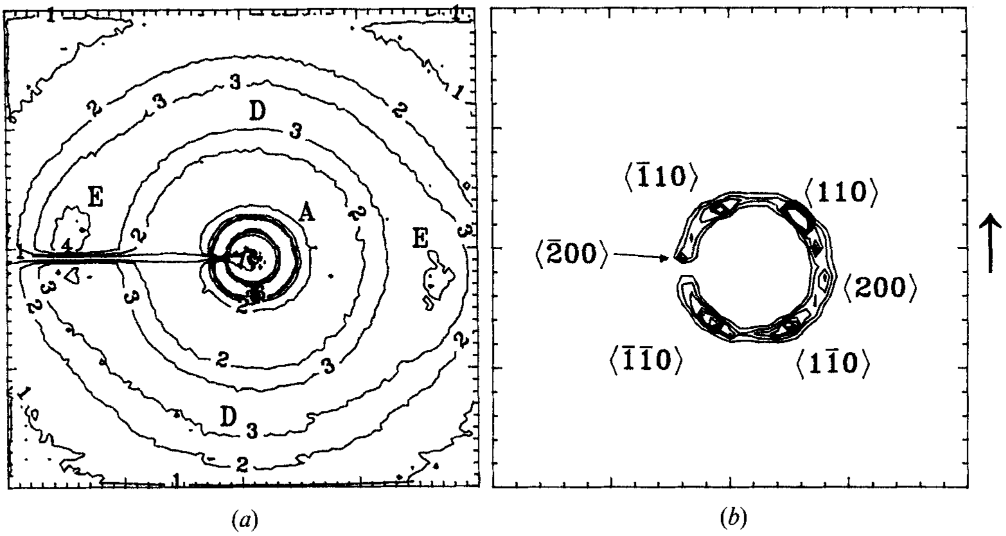

(*a*) (*b*)

Figure 11. (*a*) 'Fibre' X-ray diffraction pattern from a magnetically aligned sample of compound **6i**. The orientation of the magnetic field in relation to the diffraction pattern is shown by the direction of the arrow. A, Bragg peaks (110s/200s); E, intracolumnar peaks; and D, alkyl chain peak. (*b*) Detail from (*a*) showing orientation of 200s and 110s. The 2̄00 peak is obscured by the beamstop.

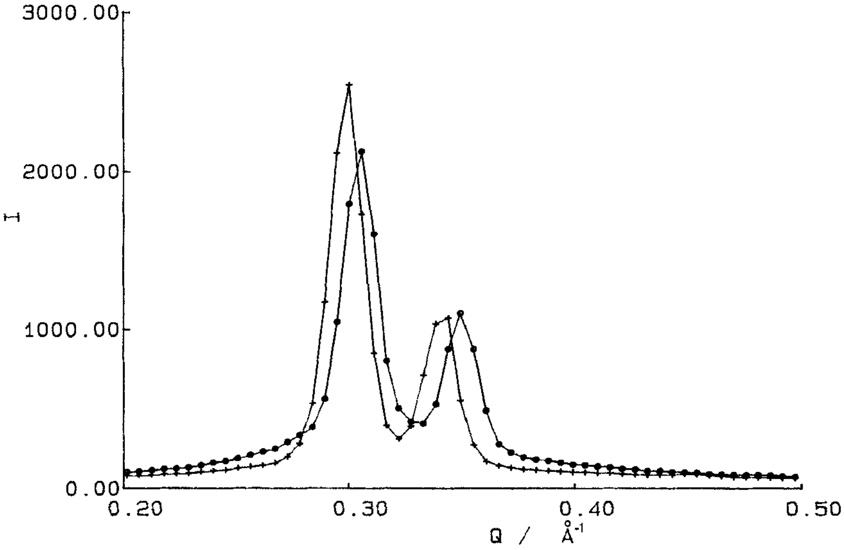

Figure 12. Small-angle diffraction peaks (200s and 110s) from compound **6i** at room temperature and 100°C. (+) Room temperature and (○) 100°C.

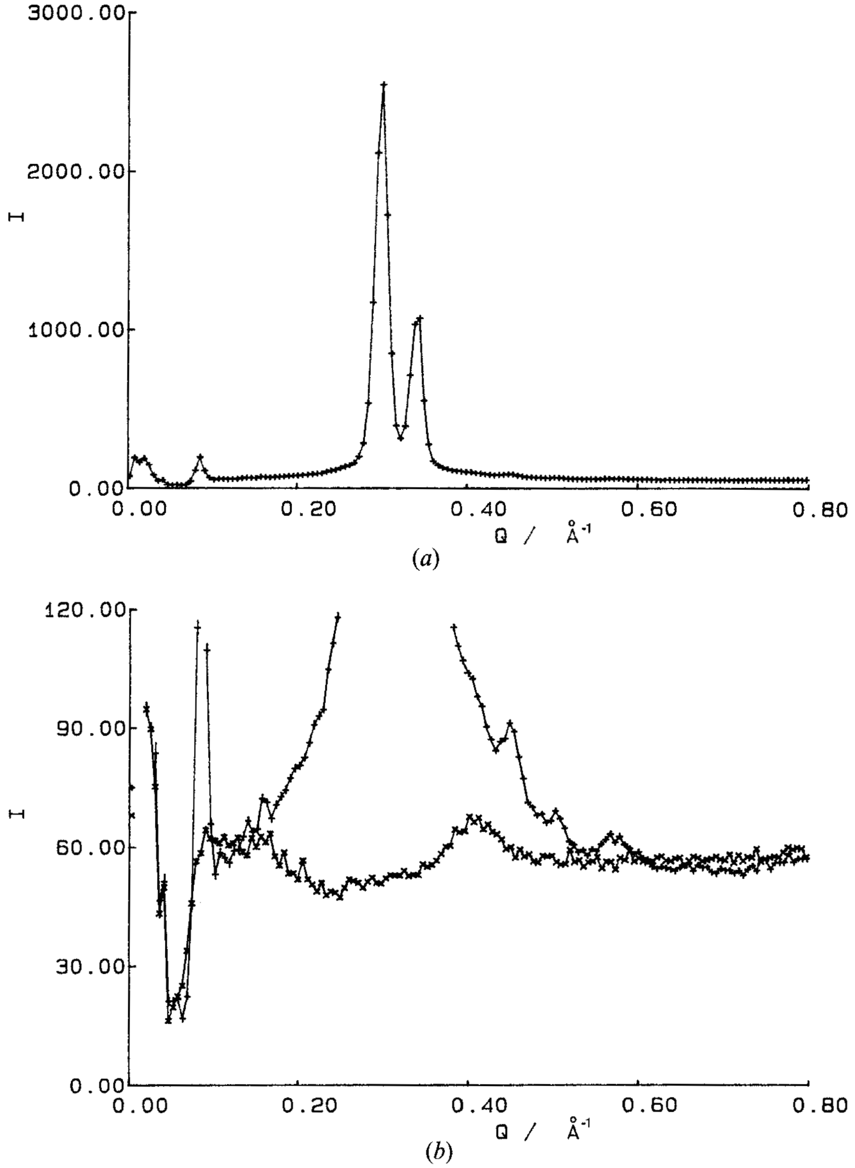

Figure 13 (*a*) X-ray diffraction from compound **6i** and (*b*) detail from (*a*) showing the 210, 020 and 310 peaks with background. (+) Sample and (×) background.

peak. Due to increased thermal motion of the molecules, not only are the 210, 020 and 310 peaks considerably weaker at 100°C than at room temperature, but there is also an increase in diffuse scattering around the 110 and 200 peaks at 100°C (see figure 12).

From figure 11, it can be shown that the sample is not a monodomain, but is a fibre-averaged sample, i.e. the column axes assume any orientation perpendicular to the aligning magnetic field (see figures 14 and 15). Figure 15 shows a 3D view of the

Table 3. Lattice parameter fitting for compound **6i** (*a*) at room temperature with $b=25{\cdot}0$ Å and $a=36{\cdot}5$ Å ($a=1{\cdot}46b$); (*b*) at 100°C with $b=24{\cdot}3$ A and $a=36{\cdot}0$ Å ($a=1{\cdot}48b$).

h	*k*	Q (calc)/Å^{-1}	Q (observed)/Å^{-1}
1	1	0·305	0·299
2	0	0·344	0·341
2	1	0·426	0·45†
0	2	0·503	0·507
3	1	0·574	0·578

(*a*)

Q (110) = 0·304, Q (200) = 0·349
Hence, $b=24{\cdot}3$ Å, $a=36{\cdot}0$ Å
No other peaks clearly visible

(*b*)

† Omitted for the purpose of fitting.

diffraction pattern in reciprocal space. The observed pattern is a vertical section through this 'space'. A monodomain sample would yield 6 sharp Bragg peaks (110/200s) and an isotropic ring associated with alkyl chain close-packing interactions at a spacing of about 4·5 Å. Fibre-averaging about b^* has the effect of 'rotating' the peaks into circles about the aligned axis and hence a fibre-averaged sample yields 2 extra broad peaks at $Q=1{\cdot}7$ Å^{-1} (3·7 Å in real space) which are connected with the intracolumnar spacing of the molecules. The distortion from a hexagonal cell is such that $a<\sqrt{3}b$, so it is likely that any tilt of the molecules with respect to the column axis is predominantly in the a direction. Since the a axis is perpendicular to the fibre axis, no splitting of this 3·7 Å peak would be expected, even if the molecules were tilted. True monodomains or fibre averages about a^* would be needed to observe

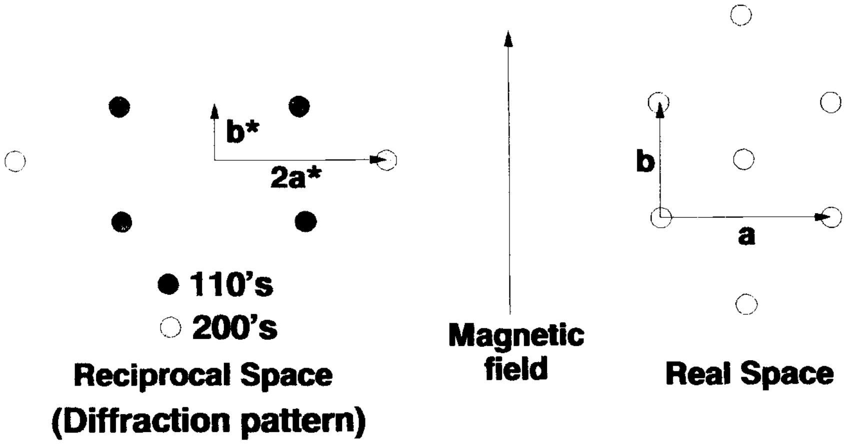

Figure 14. Schematic representation of the structure of the rectangular lattice of the mesophase formed by compound **6i** in relation to the diffraction pattern and magnetic field. The sample was slab shaped with the Kapton windows parallel to the page and the incident X-ray beam was perpendicular to the page.

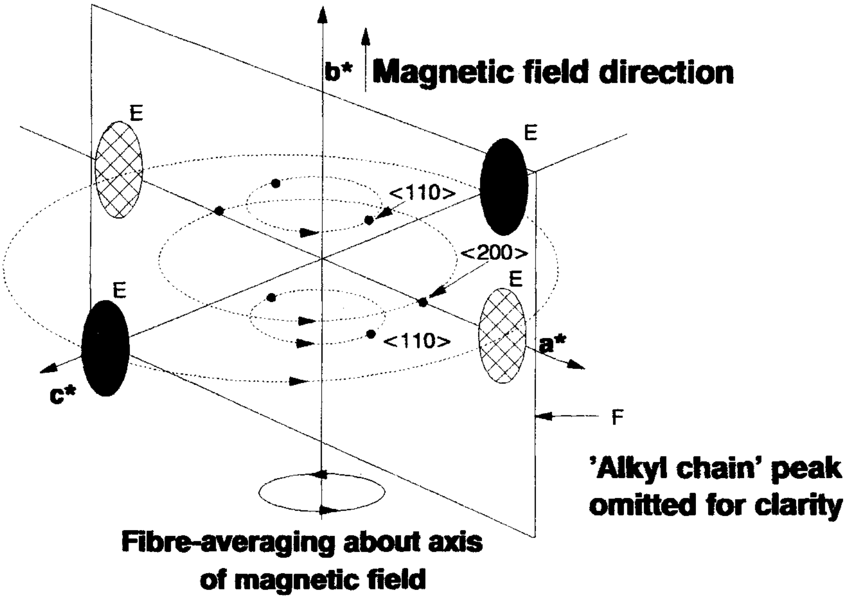

Figure 15. 3D schematic of reciprocal space showing X-ray diffraction pattern generated by fibre-averaged sample of compound **6i**. E, Intracolumnar peaks (3·7 Å); and F, section through reciprocal space (approximating to Ewald sphere) represents diffraction pattern.

directly the molecular tilt. The fibre-averaging effect is clearly visible in figure 11 (*a*) where the 3·7 Å intracolumnar peak is observed near the equator, but the 4·7 Å alkyl chain peak remains a diffuse ring.

Compound **6j** also exhibits a columnar mesophase at room temperature. Measurement of the small angle (110/200) peaks at 26°C yields lattice parameters of $b=20{\cdot}7$ Å and $a=44{\cdot}1$ Å ($a=2{\cdot}13b$). Due to the sample's small size (1–2 mg), no other peaks were observed. It is difficult to suggest why this compound forms such a pronounced rectangular lattice (i.e. pronounced distortion from a hexagonal geometry ($a=\sqrt{3}b$)) but it should be noted that the analogous 'unbranched' compound ($R=CH_2OC_6H_{13}$) also forms a rectangular lattice (see table 1).

4. Conclusion

The columnar mesophase exhibited by the octa-alkoxymethylphthalocyanine derivatives have been shown to differ from their *n*-alkyl analogues in several ways which we attribute to the more flexible ether linkage.

(i) They tend to show columnar mesophases at lower temperatures.
(ii) The discs appear to be able to approach to face to face contact at 3·7 Å and have thicker columns for the same substituent length.

With branched chains, room temperature rectangular columnar mesophases have been formed. These have been aligned by a magnetic field and the 'fibre' diffraction patterns suggest negative magnetic susceptibilities. The different azimuthal distribution of the intracolumnar and alkyl chain peaks confirms their assignments.

We would like to thank Dr R. J. Musgrove and Mr A. S. Cherodian for many helpful discussions and the SERC and the DRA-Electronics Divn, RSRE, Malvern, for financial support.

References

[1] Piechocki, C., Simon, J., Skoulios, A., Guillon, D., and Weber, P., 1982, *J. Am. chem. Soc.*, **104,** 5245.

[2] Guillon, D., Skoulios, A., Piechocki, C., Simon, J., and Weber, P., 1983, *Molec. Crystals liq. Crystals,* **100,** 275. Guillon, D., Weber, P., Skoulios, A., Piechocki, C., and Simon, J., 1985, *Molec. Crystals liq. Crystals,* **130,** 223. Guillon, D., Weber, P., and Skoulios, A., 1987, *J. phys. Chem.*, **91,** 2242. Hanack, M., Beck, A., and Lehmann, H., 1987, *Synthesis,* p. 703.

[3] Ohta, K., Jacquemin, L., Sirlin, C., Bosio, L., and Simon, J., 1988, *New J. Chem.*, **12,** 751.

[4] Masurel, D., Sirlin, C., and Simon, J., 1987, *New J. Chem.*, **11,** 455.

[5] van der Pol, J. F., Neeleman, E., Zwikker, J. W., Nolte, R. J. M., and Drenth, W., 1988, *Recl. trav. Chim. Pays-Bas,* **107,** 615. van der Pol, J. F., Drenth, W., Sluyters, J. H., and Baas, A., 1989, *J. electroanalyt. Chem.*, **271,** 41. van der Pol, J. F., Drenth, W., Neeleman, E., Zwikker, J. W., Nolte, R. J. M., Aerts, J., Visser, R., and Picken, S. J., 1989, *Liq. Crystals,* **6,** 577. Schouten, P. G., van der Pols, J. F., Zwikker, J. W., Drenth, W., and Picken, S. J., 1991, *Molec. Crystals liq. Crystals,* **195,** 291.

[6] Cho, I., and Lim, Y., 1987, *Chemistry Lett.*, p. 2107. Cho, I., and Lim, Y., 1988, *Molec. Crystals liq. Crystals,* **154,** 9.

[7] Lelievre, D., Petit, M. A., and Simon, J., 1989, *Liq. Crystals,* **4,** 707.

[8] Cook, M. J., Daniel, M. F., Harrison, K. J., McKeown, N. B., and Thomson, A. J., 1987, *J. chem. Soc. chem. Commun.*, p. 1086.

[9] Cherodian, A. S., Davies, A. N., Richardson, R. M., Cook, M. J., McKeown, N. B., Thomson, A. J., Feijoo, J., Ungar, G., and Harrison, K. J., 1991, *Molec. Crystals liq. Crystals,* **196,** 103.

[10] Cook, M. J., Cracknell, S. J., and Harrison, K. J., 1992, *J. mater. Chem.*, **1,** 703.

[11] Cammidge, A. N., Cook, M. J., Harrison, K. J., and McKeown, N. B., 1991, *J. chem. Soc./Perkin Trans. 1,* p. 3053.

[12] Bateman, J. E., Connolly, J. F., Stephenson, R., Flesher, A. C., Bryant, C. J., Lincoln, A. D., Tucker, P. A., and Swanton, S. W., 1987, *Nucl. Instrum. Meth. phys. Res. A,* **259,** 506.

[13] Destrade, C., Tinh, N. H., Gasparoux, H., Malthête, J., and Levelut, A.-M., 1979, *Third Liquid Crystal Conference of Socialist Countries,* Budapest. Destrade, C., Tinh, N. H., Gasparoux, H., Malthête, J., and Levelut, A.-M., 1981, *Molec. Crystals liq. Crystals,* **71,** 111. Destrade, C., Gasparoux, H., Foucher, P., Tinh, N. H., Malthête, J., and Jacques, J., 1983, *J. Chim. phys.*, **80,** 149.

[14] Weber, P., Guillon, D., and Skoulios, A., 1991, *Liq. Crystals,* **6,** 369.

[15] Robertson, J. M., 1936, *J. chem. Soc.*, p. 3230.

[16] Kitaigorodsky, A. I., 1973, *Molecular Crystals and Molecules* (Academic Press).

[17] Haslam, S. D. (unpublished results).